Computer Simulation of Pore–Throat Ratio on the Features of Flow Configuration of Permeability in Tightly Compressed Porous Matrix

Zulqarnen Asadullah Baloch†, Syed Baqer Shah††, Hisamuddin Shaikh†††, Mahera Erum Baloch††††

†M.U.E.T Jamshoro, Pakistan, ††, †††SALU Khairpur Pakistan, ††††I.C.E.U Duisburg-Essen,Campus Duisburg, Germany

Abstract

Present research work focuses on the two–dimensional axi symmetric incompressible flow of a constant viscosity Newtonian fluid past Pore–Throat circular pipe. Numerical solutions are obtained through time–marching finite element method. A Taylor–Galerkin/Pressure–Correction procedure in semi–implicit form is employed to achieve the steady–state solutions. To investigate the influence of inertia, such as, Reynolds number, impact of various pore–throat ratios on flow structure, pressure differential, and friction factor different parameters are employed. Predicted numerical results demonstrate Pore–Throat ratio have vital impact on the flow field distribution. Flow structure is visualized via streamline distribution, particularly formation of recirculation region in its intensity and size of vortices regarding length and position of vortex centre is analyzed by contour plots and graphs. Whilst, pressure distribution is also presented though contour plots and friction factors through graph. From the predicted numerical result, a good agreement is observed against other numerical as well as experimental solutions

Key words:

Pore–Throat Tube, Finite Element Method, Newtonian Fluids, Flow in Porous Media, Low Permeability, Pore Configuration.

1. Introduction

Flow of fluid inwardlow permeability porous matrix significantly focusednow days in the pore–scale or micro–scale process. Computational investigation of such type of flows has intent by various researchers. Porous medium and fluid as well, both are considered as continuous mediums and might be separated in to four dissimilar scales like core–scale, pore–scale, giga–scale and mega–scale (Bear, [1], Al–Raoush and Alshibli, [2]). Since problems concerned with issues of micro–scale is not fully comprehended that's why until now it's not being clearly explained and is relatively scale model.Micro–scale's time–space may differ in various fields of study. Space micro-scale is generally referred to huge scales (Harley, et al. [3] and Fu–Quan, [4]). It has from micron to atomic ranges in common such as submicron and micron; cluster and atom as well as Nano–metre even upper limit of micron is less than hundred µm. The application of micro–scale values in devices might be depend upon the scale order that enhances in a region towards volume ratios. Whilst, in case of fuel cells, mass and heat transfer or in electrochemical reactions principals of micro–scale may escort to key advancement density of power and cost effectiveness (Mala and Dong–Qing [5] and Kandlikar [6]). The submicron may beclassified as from0.1µm to 1nm in size. Scale having outsized about 1mm is considered to be macroscopic scale and having ranges between 1µm to 1 mm is considered as micro–scale (Song and Liu, [7], Hassanipour and Lage, [8], Lahbabi and Chang [9] and Pilitsis, et al. [10]).Number of researchers investigated recently on the fluid flow in the area of low permeability of porous matrix (Fu–Quan, [4], Gravesen, et al. [12], Jicheng, [12], Shaikh, et al., [13, 14] and Shah, et al.,[15, 16]).

To investigate the flow phenomena of Newtonian and non–Newtonian fluids a finite element model is developed (Shaikh, et al. [13,14]).Particularly, in non–Newtonian case, a shear thinning fluid is simulated through 1: 4 ratio of backward step channel and pipe. The Power Law model was employed to analyse the behavior of various types of fluids with changing the power law index rate. Also, different fluid inertia through flow features and different low permeability's were tested to analyse the effects of porous medium and without porous medium. The streamline patterns of the velocity, reattachment length and silent corner vortex length was computed with the increasing the fluid inertias. For Newtonian fluid, due to low fluid inertia the tinny vortex observed at silent corner of the backward step channel. As fluid inertia has been enhanced the formation of recirculation region enlarge the size of vortex was observed up to Reynolds number (Re = 50) fifty and fill the whole region of the backward step channel and pipe. For non–Newtonian fluids, the same vortex phenomena observed but the vortex size is lower than the Newtonian fluids and not filled the whole region of the backward step channel. Conversely, due to fill the porous medium the vortex phenomena vanished completely at all fluid inertias and with changing the low

Manuscript received November 5, 2018
Manuscript revised November 20, 2018

permeability rates. Only, observed the flow path lines in the channel as well as pipe.

The flow through low permeability porous material of fluid is purely referred as micro–scale flow phenomena, such as Jicheng, et al. [12] investigated the appearances of fluid flow through Expansion–contraction Channel of Low Permeability Reservoir. The two–dimensional Newtonian fluid model presented to express the flows of velocity, speed and stream functions and various computations of the models such as effects of same pore radius, various throat radius and change in pore radius were analyzed. Jicheng, et al. [12] concluded that effects of throat radius and various ratios of pore throat were highly showed the effects on the fluid flow distributions but small variations are examined with the influences of pore length.

To analyse the flow features through sinusoidal tube was investigated through time–marching finite element procedure (Shah, et al., [15, 16]). Different effects on the flow features were presented such as effect of fluid inertia and various types of undulation effects (40%, 50% and 60%). A Predicator–Corrected Taylor–Galerkin/Pressure–Correction algorithm is adopted. Different flow patterns were observed as streamlines, vortex intensity and critical position of vortex development on the function of fluid inertia. Shah [16] concluded that due to enhance the fluid inertia, the vortex centre moves towards centre of undulation and subsequently, then shifts towards downstream region. Also, more stability was perceived at the high level of undulation like 60%. Also, Shah, et al., [15,16], further investigated to demonstrate the impact of various undulation levels as well as effects of lower and higher fluid inertia and also influence of fibre suspension flows through sinusoidal tube geometry.

2. Problem Specification

Fluid within Pore–Throat tube is investigated here for incompressible Flow of Newtonian fluid. Geometry selected as computational domain of interest is circular tube and flow is assumed to be axisymmetric so the upper–half of the geometry is considered. The domain of the flow is demonstrated in Figure–1. Whereas the radius, 'r_w'of the Pore–Throat circular geometry is determined laterally in the axial flow direction as:

$$r_w = \Re_s \left[1 + \lambda Cos\left(\frac{2\pi z}{L_a} \right) \right] \quad (1)$$

Where,λ and L_a are respectively non–dimensional amplitude of Pore–Throat wave and wave length. While $\Re_s$ is an average radius of plane circular domain (straight tube with unit radius). The coordinate system considered in this investigation is cylindrical polar coordinates (r, z), where r is a radial direction and z-axis is an axial direction, along the axis of flow direction.

To state the well–posed problem, it is vital to describe both initial and as well as boundary conditions. Here mixed Dirichlet and Neumann boundary conditions considered as given in following Table–01:

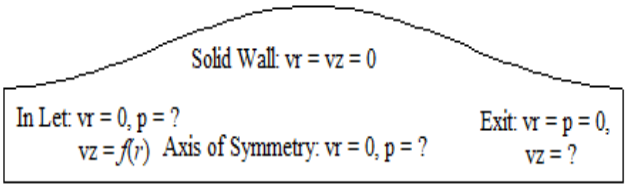

Fig. 1 COMPUTATIONAL DOMAIN OF FLOW INTEREST PORE–THROAT TUBE.

Table 1:

For Time–dependent Momentum Equation: Boundary and Initial conditions	
Boundary Conditions	1. At inlet, axial velocity component is fixed with the formula $v_z = v_{max}\left\{1-\left(\frac{r}{R_s}\right)^2\right\}$ and vanishing radial component $v_r = 0$ is considered. 2. On solid walls no-slip condition are fixed: $v_r = v_z = 0$. 3. At exit, axial velocity component v_z is free and radial component v_r and p are fixed with vanishing value. 4. At axis of symmetry, a traction free condition for radial velocity ($v_r = 0$) and $\frac{\partial v_z}{\partial r} = 0$ are fixed.
Initial Conditions	Motionless flow condition $v_r(z,0) = v_z(r, 0) = 0$

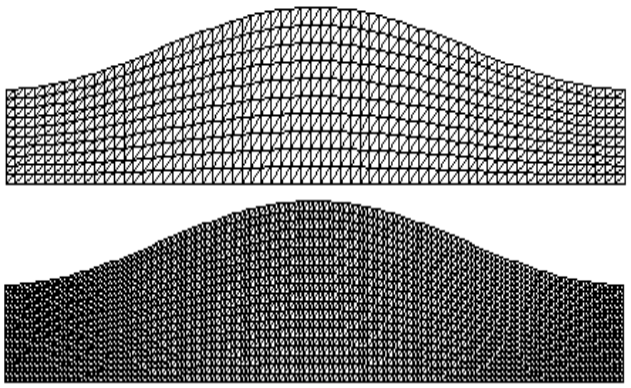

Fig. 2 FINITE ELEMENT CORE AND REFINED MESHES OF PORE–THROAT TUBE USED IN THE SIMULATION.

3. System of governing equations

This investigation considers an incompressible flow of Newtonian fluid under isothermal condition within Pore–Throat tube. The flow is governed via continuity and momentum transport equations. The dimensionless system of equations in the polar coordinate system without considering body forces can be presented as:

Continuity equation:

$$\frac{\partial v_z}{\partial z}+\frac{1}{r}\frac{\partial (rv_r)}{\partial r}=0 \tag{2}$$

Time–dependent Momentum Equation:

$$\rho\left(\frac{\partial v_r}{\partial t}+v_r\frac{\partial v_r}{\partial r}+v_z\frac{\partial v_r}{\partial z}-\frac{v_r^2}{r}\right)=\left[\frac{1}{r}\frac{\partial (rv_r)}{\partial r}+\frac{\partial v_z}{\partial z}-\frac{v_r}{r}\right]-\frac{\partial p}{\partial r} \tag{3}$$

$$\rho\left(\frac{\partial v_z}{\partial t}+v_r\frac{\partial v_z}{\partial r}+v_z\frac{\partial v_z}{\partial z}\right)=\left[\frac{1}{r}\frac{\partial (rv_r)}{\partial r}+\frac{\partial v_z}{\partial z}\right]-\frac{\partial p}{\partial z} \tag{4}$$

Where v_r and v_z are the non-dimensional velocity components of fluid material point in the radial and axial direction respectively, m/s; while, r and z are respectively radial and axial direction. Whilst ρ is the density of fluid material point, kg/m3 and t is time (s).

As per actual range of low permeability wires, three different set of parameters for Pore–Throat tube flow models are analyzed here. It is observed that, pore length and pore–throat ratio of Pore–Throat tube flow exert on the flow line and shear stress distribution (Makihara, et al. [17]). In this particular investigation feature of fluid distribution in Pore–Throat tube flow is to investigated at the conditions of different pore parameters.

4. Numerical Algorithm

For low permeability flows, atime–marching finite element method is employed to predict steady–state numerical solutions.In this regard a semi–implicit based Taylor–Galerkin/Pressure–Correction algorithm(Baloch, [18], Baloch, et al. [19] and Baloch and Memon, [20]) is employed. Initially, the scheme was developed for complex flows of Newtonian fluids with constant viscosity in the time stepping frame work(Qureshi and Baloch, [21], and Shah, et al. [15, 16]). For completeness, the summary of the algorithm is described here. At half time step, this scheme comprises discretisation of time derivative through forward difference method. Whilst, at full time step, a central difference approach is used through Taylor series. While, for pressure term, a pressure–correction technique is adopted to guarantees the second order accuracy and stability(Baloch, et al. [22, 23]).For spatial discretisation is achieved through Galerkin approach as a scheme terms in Taylor–Galerkin algorithm. For present numerical algorithm employed in this study, this approach also provides the bases to acquire the steady–state results, for further details reader are referred to previous published references (Baloch, et al. [22, 21], Shaikh, [24] and Shah, [25]).

Stage–1(a): Compute velocity field at half time–step $v^{n+\frac{1}{2}}$ for given $\left(v^n, p^n\right)$, such that

$$\left\{\left(\frac{2}{\Delta t}\left(v^{n+\frac{1}{2}}-v^n\right),v\right)+\frac{1}{2\,\mathrm{Re}}\left(\nabla\left(\left(v^{n+\frac{1}{2}}-v^n\right),\nabla v\right)\right)\right\}$$
$$=\left(-p^n-\frac{1}{\mathrm{Re}}\nabla v^n,\nabla v\right)-\left(\left((v.\nabla)v\right)^n,v\right) \tag{7}$$

Stage–1(b): Calculate non–Solenoidal velocity vector field v^*, for given $\left(v^n, v^{n+\frac{1}{2}}, p^n\right)$, such that:

$$\left\{\left(\frac{1}{\Delta t}\left(v^*-v^n\right),v\right)+\frac{1}{2\,\mathrm{Re}}\left(\nabla\left(v^*-v^n\right),\nabla v\right)\right\}$$
$$=\left(-p^n-\frac{1}{\mathrm{Re}}\nabla v^n,\nabla v\right)-\left(\left((v.\nabla)v\right)^{n+\frac{1}{2}},v\right) \tag{8}$$

Stage–2: Calculate pressure–differential $p^{n+1}-p^n$, for given, v^* and p^n, such that:

$$\left(\theta\nabla\left(p^{n+1}-p^n\right),\nabla q\right)=\frac{-1}{\Delta t}\left(\nabla v^*,q\right) \tag{9}$$

Stage–3: Determine velocity vector field at full time–step v^{n+1} for given v^{*} and $p^{n+1}-p^{n}$, such that:

$$\left(\frac{1}{\Delta t}\left(v^{n+1}-v^{*}\right),v\right)=\left(\theta\left(p^{n+1}-p^{n}\right),\nabla v\right) \tag{10}$$

5. The Numerical Solutions and Discussions

5.1 The Effect of Pore–Throat Ratio on Formation of vortices

It is assumed that the value of flow parameters in circular domain remains same, such as pore length taken equal to 2 whilst, for various Pore–Throat ratios, pore radius and throat radius are computed by above equation (01) along axial direction z. To investigate the effects of Pore–Throat ratios on flow structure, a unit maximum velocity at centre of the computational domain is fixed for all cases. Predicted solutions are demonstrated through streamline projections. Stream function is fixed according to maximum velocity at centre, while, vanishing value of stream function is fixed at solid wall of domain. Vortex intensity is computed through the difference between wall value and the stream function value in the centre of vortex. In core flow, the stream lines are plotted at the difference of 0.05, while, in recirculating region stream lines are plotted at equally spaced according to their stream function values of vortex centre.

5.2 Formation of Recirculation Flow Rate (Vortex Development)

For development of recirculating flow rate streamline projections are presented at different Pore–Throat ratios, critical Reynolds numbers are identified in the fig. 3. Where, for all Pore–Throat ratios cases, an embryo vortex develops in the upstream of the computational flow domain. At low Pore–Throat ratio of 1:2, vortices develop away from throat and before peak of pore, whereas, as Pore–Throat ratio increase the centre of the embryo vortex shift towards upstream close to upstream throat, this phenomenon of formation of recirculation flow rate is illustrated in fig. 3.When the ratio is 2, at low value of inertia the fluid velocity is in the upper part of the pore, rightclose to pore wall. As the Reynolds number is increasing, the fluid velocity in that place reduces evidently and forming vortex (Pilitsis, et al. 1991 and Fu-Quan, 2004). Whilst, in fig. 4, graph demonstrate the start of vortex development against critical Reynolds number. It is observed that at small Pore–Throat ratio of 1:2 the start of vortex development is at Reynolds number of forty (Re=40), while, for Pore–Throat ratio of 1:5, the start of vortex development is much earlier at Reynolds number equal toeleven (Re=11) with monotonically decreasing trend with increasing Pore–Throat ratio, subsequently, progresses towards asymptotic behaviour.Similarly, same trend is observed for 1:7, 1:9 and 1:11 Pore–Throat ratio. Whereas, recirculating flow rate is increasing with enhancing Pore–Throat ratio in non–linear fashion.

Three different tube models are selected in this study to investigate the effects of various Pore–Throat ratios on various flow characteristics. These Pore–Throat ratios are based on the micro–pore description of genuine reservoir. The various Pore–Throat ratios selected here are 1:2, 1:3, 1:5, 1:7, 1:9 and 1:11 respectively. Since pore radius has small effects on permeability in genuine reservoir and it is generally controlled by throat radius. More over as the pore radius has some changes in low permeability reservoir than throat radius. The précised non–dimensional parameters of each Pore–Throat flow model are obtained through above equation(1).

5.3 Characteristics of Flow Structure, Effects of Inertia

In fig. 5, streamline patterns are plotted at Re = 100 shows the flow structure of different Pore–Throat ratios. One can see that, with increasing Pore–Throat ratio a strong recirculating region develops in the centre of pore. As Pore–Throat ratio increases vortex enhancement is observed and strengthening the vortex intensity. Whereas, vortex centre is moving from upstream of pore pushing towards downstream of pore in the vicinity of exit throat. When the Pore–Throat ratio is 1:2, the flow only exists in the vicinity of central line (axis of symmetry) parallel to the throat radius and the fluid velocity at other points in pore is very slow nearly vanishes. Whilst, centre/core flow close to axis of symmetry increases. From stream function's physical significance (the difference in stream function of any two streamlines in plane flow field is equal to volume flow rate per unit thickness), if the ratio is larger, stream function figure is smaller and distance of two adjacent streamlines is smaller. It also represents that if fluid influx and fluid velocity are small, then the volume of relevant fluid passing through the pore space is small. On the view of stream function, one of the reasons which lead to low sweep efficiency in low permeability layer is large Pore–Throat ratio and small effective volume of injected fluid (Balhoff, [26] and Al-Raoush and Alshibli, [2]).

5.4 Characteristics Behavior of Pressure Differential Distribution

In fig. 6, the graph of the scaled pressure differential is plotted at Re = 100 with increasing Pore–Throat ratio (on left). Fluid pressure differential is scaled through straight tube of same length. It is clear from the fig. 6 (on left), that as the Pore–Throat ratio is enhanced, the scaled fluid's pressure differential increases monotonically. At low Pore–Throat ratio, scaled pressure differential slowly increase, whereas, at comparatively high Pore–Throat ratio, scaled pressure differential is increasing rapidly and display exponential tendency. Whilst, at critical Reynolds number, the scaled pressure differential is displayed infig. 6 (on right) exhibits reverse phenomena, i. e., with increasing inertia the scaled pressure differential drops at lowest Pore–Throat ratio, whilst, pressure differential is higher at low value of inertia and larger Pore–Throat ratio. Scaled pressure differential exhibits monotonic decreasing tendency, whereas, at comparatively at higher Reynolds number and lower Pore–Throat ratio the scaled pressure differential approaches to asymptotic state (Lahbabi, and Chang, 1986). In fig. 7, pressure isobars are plotted for Re = 100 with increasing Pore–Throat ratio. It clearly shows that as Pore–Throat ratio is augmented from 1:2 to 1:11, fluid entre from straight tube with unit radius into the first throat, fluid release the pressure inside pore, subsequently, pushes the fluid in the second throat and again it releases in the downstream straight tube. For all selected flow model of Pore–Throat pipe at upstream pressure differential increases, whilst, at downstream section it decreases even go in reverse/negative direction.

6. Conclusion

To seek the steady–state numerical solutions a Taylor–Galerkin/Pressure–Correction Scheme is adopted. Numerically computed predictions are compared against other numerically obtained solution and experimental results. Effects of Pore–Throat ratio and influence of inertia (Re) on pressure differential and flow structure investigated. Enhancement of vortices (Qv) at various Reynolds number is especially focused. The vortex enhancement (Qv) at different Reynolds number is especially focused. For different Pore–Throat ratio and fluid inertia (Re), start of embryo recirculation region is identified to realise "Critical Reynolds number".

Distinguished calculations of 1:2, 1:3, 1:5, 1:7, 1:9 and 1:11 Pore–Throat rations separately, it is concluded that when the ratio increase or throat radius reduced and pore radius increase, then internal–pore velocity of fluid will decrease and a recirculating region develops. This recirculating region grows and occupies large area of pore region, subsequently, strengthening the vortex intensity at high value of inertia and almost grapes whole pore region. Whereas, in core flow, the velocity of the fluid increases with increasing inertia. Predicted solutions illustrate the association between recirculating flow–rate and pressure differential appearing in agreement with Navier–Stokes equations.

Acknowledgement

Authors would like to thanks the Institute of Environment Engineering and Management, Mehran University of Engineering and Technology, Jamshoro, Institute of Computer Engineering, University of Duisburg-Essen, Campus Duisburg, Germany and Department of Mathematics, Shah Abdul Latif University, Khairpur, Pakistan, for providing the opportunity to carry out this research work and computing facility.

References

[1] Bear, J., 1988, "Dynamics of Fluids in Porous Media", New York, Elsevier, 1972, (reprinted by Dover Publications).

[2] Al–Raoush, R. and Alshibli, K. A., 2006, "Distribution of Local Void Ratio in Porous Media Systems from 3D X–Ray Micro Tomography Images", J. Physica A: Statistical Mechanics and its Applications, 361(2), pp. 441–456.

[3] Harley, J. C., Huang, Y. F. and Bau, H. H., 1995, "Gas Flow in Micro–Channels", J. Fluid Mech., Vol. (284), pp. 257–274.

[4] Fu–Quan, S., 2004, "Research of the Size Effect of Liquid Flow in Low Permeability Porous Media and Micro–channels", J. Nature Magazine, Vol. 26(3), pp. 128–131.

[5] Mala, G. M. and Dong-Qing, L., 1999, "Flow Characteristics of Water in Micro Tubes", Int. J. of Heat and Fluid Flow, Vol. (20), pp. 142–148.

[6] Kandlikar, S. G., 2002, "Fundamental Issues Related to Flow Boiling in Mini Channels and Micro Channels", J. Exp. Therm. Fluid Sci., Vol. 26, pp. 38–47.

[7] Song, R. and Liu, J., 2014, "Advances in Microscopic Pore Structure
Modelling of Rock", J. of EJGE, china, Vol. 19.

[8] Hassanipour, F. and Lage, J., 2007, "The Effect of a Porous Medium on the Flow of a Liquid Vortex", Int. J. Eng., 3(6), pp. 587–596.

[9] Lahbabi, A. and Chang, H. C., 1986, "Flow in periodically Constricted Tubes: Transition to Inertial and Unsteady Flows", J. Chemical Engineering Society, Vol. 41, pp. 2487–2505.

[10] Pilitsis, S., Souvaliotis, A., and Beris, A. N., 1991, "Viscoelastic Flow in a Periodically Constricted Tube: The Combined Effect of Inertia, Shear Thinning and Elasticity", J. Rheology, Vol. 35(4), pp. 605–646.

[11] Gravesen, P., Branebjerg, J. and Jensen, O. S., 1993, "Micro Fluidics–A Review", Journal of Micromechanics and Micro engineering, Vol. (3), pp. 168–182.

[12] Jicheng, Z., Guixue, Q., Wenzhi, M. U. and Kaoping, S., 2010, "Investigation on the Characteristics of Flow in Expansion–Contraction Channel of Low Permeability Reservoir", Journal of Physical and Numerical Simulation of Geotechnical Engineering, DOI: 10. 5503/J. PNSGE. 2010.

[13] Shaikh, H., 2016, 'Numerical Simulation of Expansion and Contraction Flow in Channel Filled with and Without Porous Media', Ph. D. Thesis, Department of Mathematics, Shah Abdul Latif University, Khairpur, Sindh.

[14] Shaikh, H. Shah, S. B., Solangi, M. A. and Baloch, A., 2013, "Effects of Local Inertia in the Expansion Channel Filled with Porous Media: A Finite Element Analysis", Sindh Univ. Res. Jour. (Sci. Ser.), Vol. 45(2), pp. 207–212.

[15] Shah, S. B., Shaikh, H, Solangi, M. A. and Baloch, A., 2013, "Numerical Simulation of Flow through a Periodically Constricted Tube: Effects of Inertia and Undulation on Flow Structure" Sindh Univ. Res. Jour. (Sci. Ser.) Vol.45 (1), pp. 35– 40.

[16] Shah, S. B., Shaikh, H, Solangi, M. A. and Baloch, A., 2014," Computer Simulation of Fibre Suspension Flow through a Periodically Constricted Tube" Punjab University Journal of Mathematics, Vol. 46(2) pp. 19-34.

[17] Makihara M., Sasakura K. and Nagayama A., 1993, "Flow of liquids in micro–capillary tube consideration to application of the Navier Stokes equations", J. of the Japan Society of Precision Engineering / Seimitsu Kogaku Kaishi, 59 (3), pp. 399–404.

[18] Baloch, A., 1994. Numerical Simulation of Complex Flows of Now–Newtonian Fluids, PhD Thesis, University of Wales, Swansea, UK.

[19] Baloch, A., Townsend, P. and Webster, M. F., 1995, "On the Simulation of Highly Elastic Complex Flows", J. Non–Newtonian Fluid Mech., Vol. 59(2/3), pp. 111–128.

[20] Baloch, A., and Memon A. S., 2007, "Simulation of Corrugated Tube Flow of Non–Newtonian Fluids", MUETJET, Vol. 26(1), pp. 19–32.

[21] Qureshi, A. L., and Baloch, A., 2013, "Finite Element Simulation of Suspended Sediment Transport: Development, Validation of Application to Photo minor, Sindh, Pakistan", Advances in River Sediment Research, Fukuoka, et al. (Eds.), Taylor and Francis Group, London, pp. 1825–1832.

[22] Baloch, Z. A. K., Baloch, M. E., Shaikh, H. and Shar, M. A., 2013, "Computer Simulation of Lid Driven Shallow Cavity Flows: Effects of Fluid Inertia and Aspect Ratios", Sindh Univ. Res. Jour. (Sci. Ser.), Vol.45 (2), pp. 277–280.

[23] Baloch, Z. A. K., Baloch, M. E., Memon, R. A. and Shaikh, H., 2014, "Computer Simulation of Lid Driven Deep Cavity Flow" , Sindh Univ. Res. Jour. (Sci. Ser.), Vol.46 (4),pp. 457–460.

[24] Shaikh, H. Shah, S. B., Solangi, M. A. and Baloch, A., 2012, "Computer Simulation of Flow of Newtonian Fluid through Backward Step Channel", Sindh Univ. Res. Jour. (Sci. Ser.) Vol.44 (4) 703-708.

[25] Shah, S. B., 2017, "Numerical Simulation of Complex Flows of Fibre Reinforced Composites" Ph. D. Thesis, Department of Mathematics, Shah Abdul Latif University, Khairpur, Sindh.

[26] Balhoff, M., 2000, "Modelling the Flow of Non–Newtonian Fluids in Packed Beds at the Pore Scale", Ph.D. thesis in the department of Chemical Engineering Southfield, Michigan.

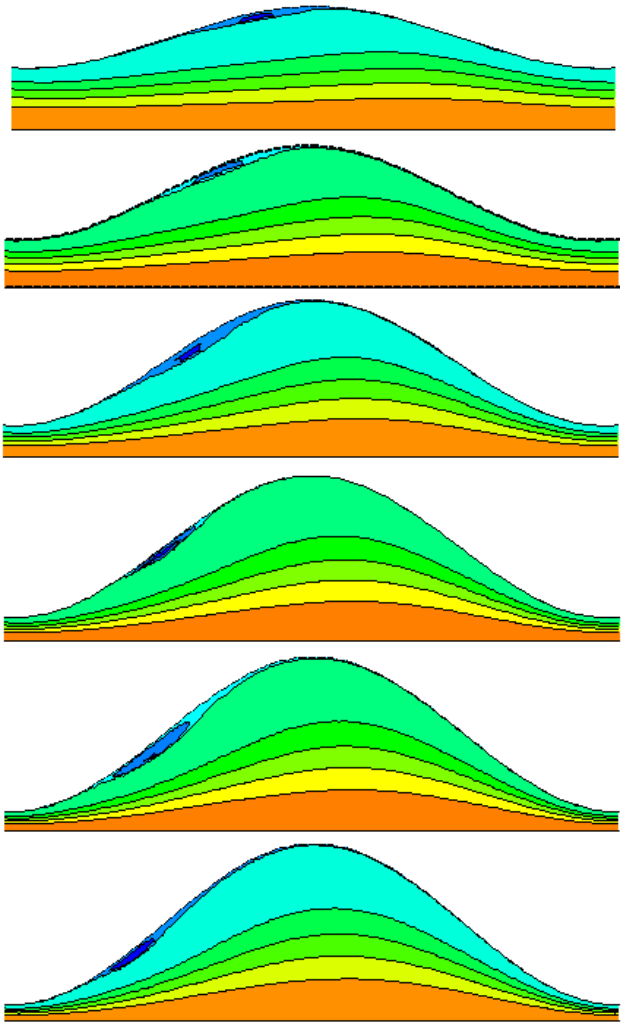

Fig. 3 COLOUR STREAMLINE CONTOURS OF FORMATION OF VORTEX OF AXISYMMETRIC PORE–THROAT PROBLEM, WITH INCREASING PORE–THROAT RATIO (FROM TOP TO BOTTOM 1:2, 1:3, 1:5, 1:7, 1:9 AND 1:11) WITH DECREASING INERTIA (FROM TOP TO BOTTOM Re = 40, 18, 11).

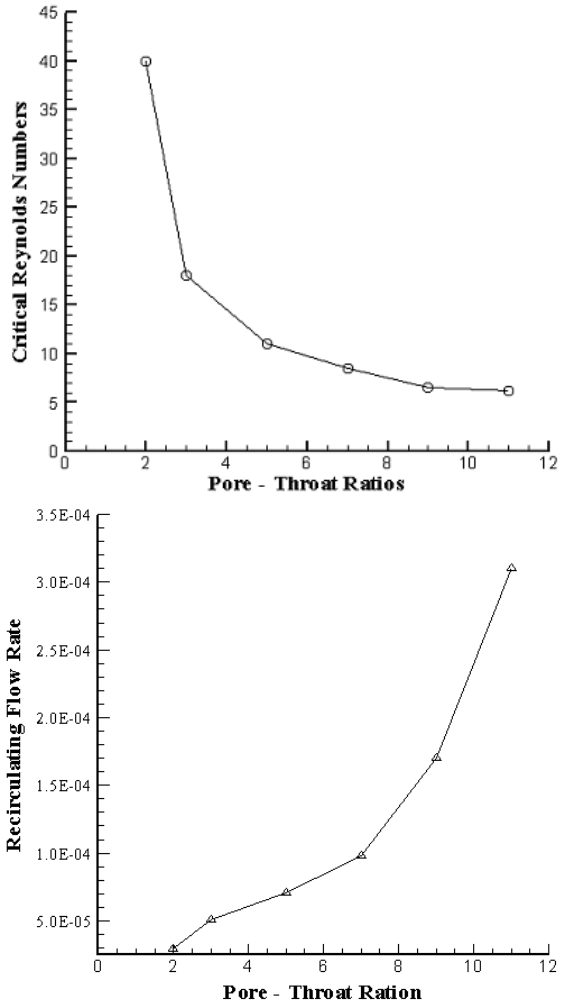

Fig. 4 GRAPH OF VORTEX DEVELOPMENT OF AXISYMMETRIC PORE–THROAT PROBLEM, WITH INCREASING PORE–THROAT RATIO AGAINST DECREASING CRITICAL REYNOLDS NUMBER (LEFT) AND RECIRCULATING FLOW RATE (RIGHT).

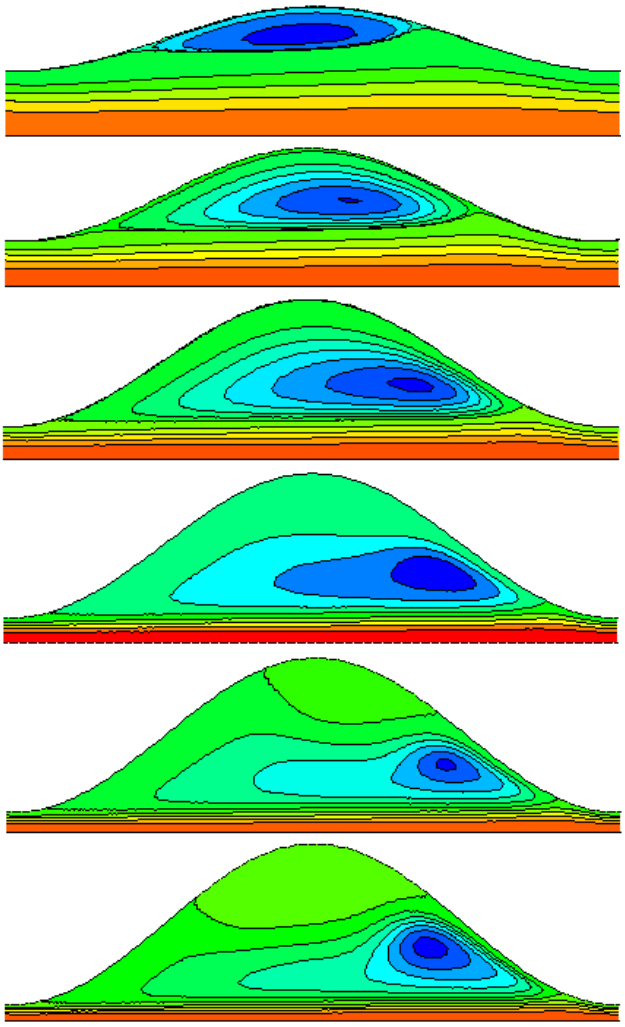

Fig. 5 COLOUR STREAMLINE PROJECTION OF AXISYMMETRIC PORE–THROAT PROBLEM AT Re = 100, WITH INCREASING PORE–THROAT RATIO FROM TOP TO BOTTOM (1:2, 1:3, 1:5, 1:7, 1:9 AND 1:11).

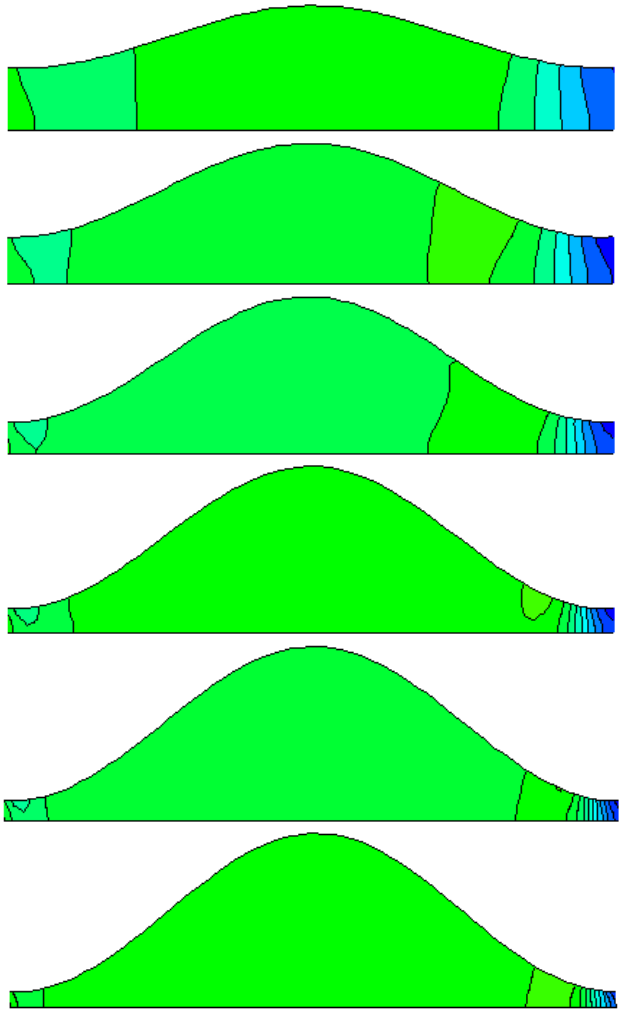

Fig. 6 COLOUR PRESSURE CONTOURS OF AXISYMMETRIC PORE–THROAT PROBLEM AT INERTIA Re = 100, WITH INCREASING PORE–THROAT RATIO (1:2, 1:3, 1:5, 1:7, 1:9 AND 1:11).

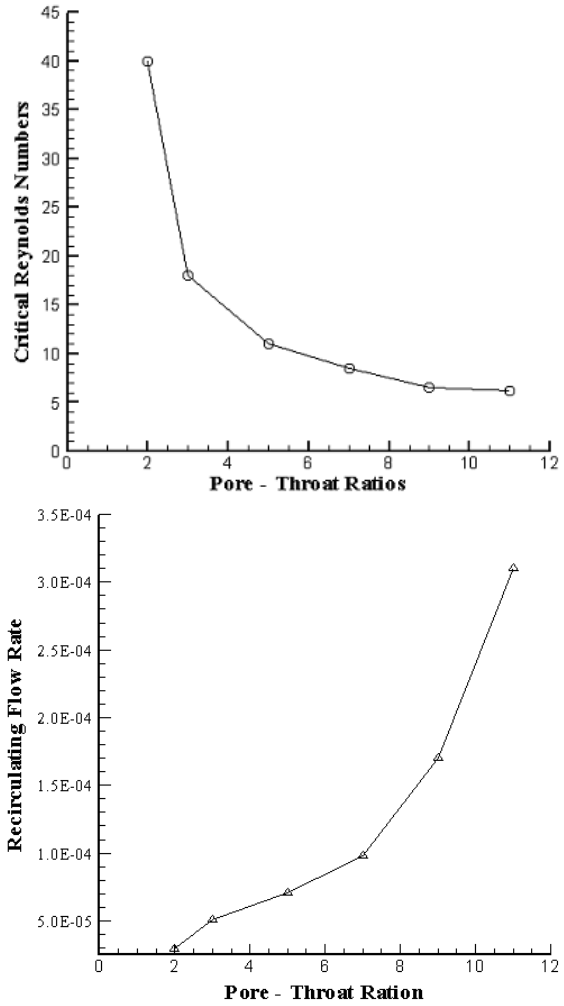

Fig. 7 GRAPH OF VORTEX DEVELOPMENT OF AXISYMMETRIC PORE–THROAT PROBLEM, WITH INCREASING PORE–THROAT RATIO AGAINST DECREASING CRITICAL REYNOLDS NUMBER (LEFT) AND RECIRCULATING FLOW RATE (RIGHT).

ZULQARNAIN ASADULLAH BALOCH
Research Scholar
M.U.E.T Jamshoro, Hyderabad,
Institutional Research and Quality Enhancement Cell Officer at SZABIST Hyderabad.

Dr. HISAMUDDIN SHAIKH
Associate Professor,
Chairman,
Department of Mathematics
Shah Abdul Latif University Khairpur

Dr. SYED BAQER SHAH
Associate Professor,
Department of Mathematics
Shah Abdul Latif University Khairpur